HHS Public Access

Author manuscript

Neuroimage. Author manuscript; available in PMC 2021 May 21.

Published in final edited form as:

Neuroimage. 2021 May 15; 232: 117893. doi:10.1016/j.neuroimage.2021.117893.

The neurocognitive correlates of brain entropy estimated by resting state fMRI

Ze Wang, PhD

Department of Diagnostic Radiology and Nuclear Medicine, University of Maryland School of Medicine, 670 W. Baltimore St, Baltimore, MD 20201

Abstract

Resting state brain activity consumes most of brain energy, likely creating and maintaining a reserve of general brain functionality. The latent reserve if it exists may be reflected by the profound long-range fluctuations of resting brain activity. The long-range temporal coherence (LRTC) can be characterized by resting state fMRI (rsfMRI)-based brain entropy (BEN) mapping. While BEN mapping results have shown sensitivity to neuromodulations or disease conditions, the underlying neuromechanisms especially the associations of BEN or LRTC to neurocognition still remain unclear. To address this standing question and to test a novel hypothesis that resting BEN reflects a latent functional reserve through the link to general functionality, we mapped resting BEN of 862 young adults and comprehensively examined its associations to neurocognitions using data from the Human Connectome Project (HCP). Our results unanimously highlighted two brain circuits: the default mode network (DMN) and executive control network (ECN) through their negative associations of BEN to general functionality, which is independent of age and sex. While BEN in DMN/ECN increases with age, it decreases with education years. These results demonstrated the neurocognitive correlates of resting BEN in DMN/ECN and suggest resting BEN in DMN/ECN as a potential proxy of the latent functional reserve that facilitates general brain functionality and may be enhanced by education.

Keywords

brain entropy; brain reserve; resting state fMRI; default mode network; executive control network; fluid intelligence

Introduction

The human brain is a dynamic system with large-scale ongoing fluctuations. Understanding these fluctuations is essential to understanding the individual differences of brain function, functional anatomy, and the pathologies associated with neuropsychiatric conditions. Both theoretical models and neuroscience experiments have demonstrated a characteristic self-

ze.wang@som.umaryland.edu.

Conflict of interest: none

Data availability statement: the HCP data is freely available from the HCP consortium. The brain entropy mapping tool is freely available from our website.

Ethics approval statement: data reanalysis has been approved by IRB. Patient consent forms were obtained by HCP.

organized criticality of normal brain activity (Deco and Jirsa, 2012; Rubinov et al., 2011). A crucial aspect of this criticality is the emergence of long range temporal correlations (LRTC)—correlations across a large time scale, meaning that signal fluctuations at one moment can influence signal up to several minutes in a future moment(He, 2011). LRTC has been postulated to relate to consciousness (Tagliazucchi et al., 2016) and high-order brain functions such as memory, attention, perception, coordination, etc (Buzsáki and Draguhn, 2004; Dean et al., 2012; Pesaran et al., 2002; Saleh et al., 2010; Thut et al., 2012; Womelsdorf et al., 2006). According to the "Communication Through Coherence" model (Fries, 2005, 2015), temporal neuronal coherence is fundamental to effective connectivity or neuronal communications. This model has been well supported by experimental results(Fries, 2015). For example, Teki et al. (Teki et al., 2013) showed that human listeners are remarkably sensitive to temporally coherent audio signals despite of the background noise and Lu et al. (Lu et al., 2017) reported that temporal coherence can rapidly reshape inter-neuron connections. The same model also predicts that the absence of temporal coherence will induce random phase of the excitability cycle of the neuron and will result in lower effective connectivity. Accordingly, improve the temporal coherence may improve connectivity and brain function as recently evidenced in (Reinhart and Nguyen, 2019). However, there still lacks a clear view of how the temporal coherence especially the LRTC is related to neurocognition across the entire brain cortex.

Using resting state fMRI (rsfMRI), we have recently proposed a method (Wang et al., 2014) to map brain entropy (BEN). While the nonparametric entropy metric, the Sample Entropy (Richman and Moorman, 2000) was used in the original paper and the accompanying software package, entropy of brain activity, the so-called BEN can be calculated using other entropy measures as we piloted in(Wang, 2012a, b). Entropy provides an approximate way to quantify LRTC through the statistical dependencies or order implicit in itinerant dynamics, expressed over extended periods of time. BEN has been shown to be independent of regional perfusion and the amplitude of low frequency fluctuations (ALFF) of rsfMRI (Zang et al., 2007) in most parts of the brain cortex (Donghui Song, 2019), suggesting that BEN may be a special property of brain activity that can not be fully characterized by regional perfusion and other resting brain activity indices such as ALFF. BEN has been shown to be reproducible across two different acquisition times and sensitive to various brain diseases and to focal neuromodulations (Song et al., 2018; Wang et al., 2014; Xue et al., 2019; Zhou et al., 2016). While these data clearly showed the potential of BEN and subsequently LRTC as a unique brain signature for studying brain diseases or normal brain conditions, its relationship or associations with neuro-cognition remain unclear.

The purpose of this study was to address the above question by leveraging the large rsfMRI and behavioral data from the human connectome project (HCP) (Van Essen et al., 2013). Based on the following literature review and abstraction, we postulated that LRTC of resting brain activity is related to a latent brain functionality reserve or alternatively speaking the general cognitive capability. Brain reserve is a well-studied model for describing the general cognitive sustainability or resilience to structural brain damages or degenerations(Stern et al., 2018). It is non-specific to any overt brain function and should be an ongoing process that would need lot of energy to maintain. The task-independent self-organized resting brain activity may actually represent the activity for generating or maintaining the latent brain

function reserve because it consumes most of brain energy and has been postulated to have a role in facilitating overt brain functions (Raichle, 2015; Raichle and Gusnard, 2005; Raichle et al., 2001; Raichle and Snyder, 2007). Accordingly, characterizing the self-organization or LRTC, a prominent property of the resting state brain activity, may provide a way to assess the latent brain reserve with higher LRTC (lower BEN) indicating a bigger or stronger reserve. The capacity of brain reserve was measured by education years and general cognitive capability. Education years is a widely used proxy for brain reserve (Stern et al., 2018) and has been validated in many studies (Albert et al., 1995; Ganguli et al., 1991; Stern et al., 1994; Valenzuela and Sachdev, 2006). Education has been shown to be moderately correlated with general intelligence (Ritchie and Tucker-Drob, 2018). In a recent study based on data from normal healthy elderly people, we have found a negative correlation between BEN in DMN and educations years(Wang, 2020). The BEN vs education association study in this paper can be considered an extension study in young health controls. The other index of brain reserve, the general cognitive capability was measured by fluid intelligence and performance of various functional tasks. Fluid intelligence is the capability for solving newly encountered problems for which learned and specialized skills provide little benefit (Horn and Cattell, 1967). In other words, fluid intelligence reflects the general functional capability of each individual, which is independent of skills and knowledge learned through education or experiences. We included several functional task performance measures in order to show the non-specificity of BEN to overt brain functions.

Based on the non-specificity and generalizability of resting state brain activity and the corresponding LRTC/BEN, we expected to see the potential LRTC vs brain reserve correlation in two “default” regions: the fronto-parietal the default mode network (DMN) (Raichle et al., 2001) and the executive control network (ECN) (also called task positive network in (Shulman et al., 1997)). Associations of the fronto-parietal networks with fluid intelligence has been described by the Parieto-Frontal Integration Theory (P-FIT) (Jung and Haier, 2007). P-FIT was abstracted from a large number of neuroimaging studies and has been supported by brain lesion studies (Woolgar et al., 2010) and proposed the prefrontal and parietal cortex as an integrated neural circuit for general intelligence and broad cognitive capabilities. Our study differed from the previous P-FIT studies by using rsfMRI and a large cohort. DMN and ECN have been more widely studied in rsfMRI literature and have been repeatedly demonstrated to be active either during task performance (G. L. Shulman, 1997; Shulman et al., 1997) or at rest (Beckmann et al., 2005; Greicius et al., 2003). This ongoing nature suggests an intensive involvement of the two regions in general functionality and subsequently the latent brain reserve. Given the above rationales and literature overview, our hypotheses were: resting LRTC in DMN/ECN is positively correlated with education years and general cognitive capacity as reflected by fluid intelligence and functional task performance.

Each rsfMRI scan from HCP contains 1200 timepoints, which is much longer than a typical rsfMRI time series acquired with the traditional single-slice excitation based echo-planar imaging sequence and provides an unprecedent an opportunity to assess the temporal behavior of BEN. Accordingly, the second aim of this study was to investigate how stable is resting BEN across different times and how the temporal dynamics of BEN relate to neurocognition.

Materials and Methods

Ethics statement

Data acquisition and sharing have been approved by the HCP parent IRB. Written informed consent forms have been obtained from all subjects before any experiments. This study re-analyzed the HCP data and data Use Terms have been signed and approved by the WU-Minn HCP Consortium.

Data and BEN mapping.

rsfMRI data, demographic data, and behavior data from 862 healthy young subjects (age 22–37 yrs, male/female=398/464) were downloaded from HCP. The mean and the standard deviation of education years were 14.86±1.82 yrs. The range of education years was 11–17 yrs. These data were released on July 21 2017. The rsfMRI data were the extended processed version. Each subject had four resting scans acquired with the same multi-band sequence(Moeller et al., 2010) but the readout directions differed: readout was from left to right (LR) for the 1st and 3rd scans and right to left (RL) for the other two scans. The alteration of phase encoding scan direction was used in order to compensate the long scan time induced image distortion. MR scanners all present field strength (B0) inhomogeneity, which causes signal distortion because of the imperfect excitation using the radiofrequency pulses that are tuned to the frequency determined by the ideal B0. While the B0 inhomogeneity caused distortions can be well corrected using two additionally acquired calibration scans using the opposite phase encoding directions: one is with LR and the other is with RL, HCP acquired two LR and two RL rsfMRI scans for the purpose of assessing the potential residual effects after the distortion correction and to assess the test-retest stability of rsfMRI measure. Each scan had 1200 timepoints. Other acquisition parameters for rsfMRI were: repetition time (TR)=720 ms, echo time (TE)=33.1ms, resolution 2×2×2 mm^3. The pre-processed rsfMRI data in the Montreal Neurological Institute (MNI) brain atlas space were downloaded from HCP and were smoothed with a Gaussian filter with full-width-at-half-maximum = 6mm to suppress the residual inter-subject brain structural difference after brain normalization and artifacts in rsfMRI data introduced by brain normalization. BEN mapping was performed with BEN mapping toolbox (BENtbx) using the default settings (Wang et al., 2014). To cope with the huge computation required to calculate BEN for the 4×860 long rsfMRI scans, we implemented the BEN mapping algorithm in C++ using CUDA (the parallel computing programming platform created by Nvidia Inc). Four graphic processing unit (GPU) video cards were used to further accelerate the process. Entropy value was calculated using the approximate entropy formula, the Sample Entropy, which is the “logarithmic likelihood” that a small section (within a window of a length ‘m’) of the data “matches” with other sections will still “match” the others if the section window length increases by 1 (see Fig. 1B). “Match” is defined by a threshold of r times standard deviation of the entire time series. Window length m is widely set to be from 2 to 3. The embedding vector matching cut-off should be selected to avoid “no matching” (when it is too small) and “all matching” (when it is too big) (Richman and Moorman, 2000). Both parameters have been assessed in previous publications (Chen et al., 2005) (Wang et al., 2014). In this study, the window length was set to be three and the cut-off threshold was set to 0.6 based on the original BEN mapping paper (Wang et al., 2014). The

entire process is illustrated in Fig. 1B. To calculate SampEn for a time series of length L, all possible data segments, each with a length of m are extracted as illustrated by the colored rectangles overlaid on the time series and the associated arrows in Fig. 1B. For the i-th data segment, its Chebyshev distance to another segment is calculated. If the distance is smaller than the cutoff threshold r, it is considered as a "match". For the segment match window length of m, the total number of matches among all possible embedding vectors is recorded (Fig. 1B.1), which is then repeated after increasing m by 1 so the segment matching window becomes m+1 (see Fig. 1B.2). SampEn is then calculated as the natural logarithm of the ratio between the total number of matches of the window length m and that of the window length of m+1 (Fig. 1C).

Fluid intelligence and functional task performance

Fluid intelligence is a measure for higher-order relational functionality for solving problems in novel situations independent of acquired knowledge(Cattell, 1963). Fluid intelligence is commonly measured using the non-verbal Raven's Progressive Matrices (Raven, 2000). In HCP, a shortened Raven's test included in the Penn Matrix Test (Bilker et al., 2012) was used. This shortened version contains 24 items. In each test item, the participant must select with the mouse on the square out of the five choices which he/she thinks best completes the missing part of a pattern. This task is independent of language, reading, and writing skills. Finding the right missing part purely depends on abstract reasoning and logic thinking rather than any learned skills or knowledge.

Task performance was measured by the accuracy of button selection during the on-magnet fMRI-based working memory, language, and relational tasks(Barch et al., 2013). The working memory task(Drobyshevsky et al., 2006) contained blocks of trails each consisting of pictures of tools, places, faces, and body parts. Within each run, the four categories of images were presented in separate blocks. Half of the blocks use a 2-back working memory task (subjects were instructed to respond 'target' whenever the current picture is the same as the one two back) and half use a 0-back working memory task. The total number of correct button press was used as the working memory task performance. The language task (Binder et al., 2011) contained two runs that each interleave four blocks of story task and four blocks of a math task. At the end of each block, subjects were instructed to finish forced-choice questions. The total number of correctly answered questions was used as the task performance. The relational task was to show a pair of objects on the top and another pair on the bottom of the screen and ask the participants to check whether the shape or texture differed across the top pair and then decide whether the bottom pair differed along the same dimension (shape or texture). The total number of correct answers was used as the task performance in this study.

A sliding window based dynamic BEN mapping.

In static BEN mapping, SampEn at each voxel is calculated from the entire rsfMRI time series. In dynamic BEN mapping, entropy is calculated at each timepoint within the sliding window with a length of L. This process can be split into two steps. As illustrated in Fig. 1, the first step is to locate the continuous neighborhood with a length of L points for each time point of the entire time series (Fig. 1A); the second step is the same as what we described

above for the static BEN mapping (or SampEn) calculation (Fig. 1B and 1C). SampEn calculated from the current L time points will be treated as the SampEn of the current time point. This process is repeated until all time points of the entire rsfMRI time series is sequentially assessed or the sliding window reaches the end of the entire time series. After all repetitions, a time series of SampEn will be produced. Note that if the sliding window length L is set to be the same as the data length of the entire time series, the above dynamic SampEn calculation will be same as the traditional static SampEn calculation.

The length of each rsfMRI scan was 1200. Because BEN mapping using rsfMRI data with a length from 120 to 200 has been shown to provide reliable results, we chose the sliding window length L to be 300 to get reliable transit BEN from each 300 timepoints rsfMRI sub-series. Successive sub-series were gapped by 9 timepoints to reduce the total number of sub-series to reduce the total computation burden. This gap was empirically set to be 9 timepoints so the interval was 9TRs=6.48 sec, which was roughly the same as one hemodynamic response function cycle. Bigger gap than 9 produced similar mean BEN maps though the variation was slightly different. Similar to the static BEN mapping mentioned above, we implemented the dynamic BEN mapping algorithm in C++ and the CUDA programming environment. GPU computing was used for finding the number of matched vectors for many voxels simultaneously. The number of voxels to be processed simultaneously was determined based on the available computation resource in the GPU card. Four Nvidia 1080Ti GPU cards were used. For each subject, four dynamic BEN time series were calculated (one for each rsfMRI scan). For each dynamic BEN time series, the mean and standard deviation (STD) as well as the coefficient of variance (CV) were calculated at each voxel. The corresponding mean, STD, and the CV maps were averaged across the first LR and the first RL rsfMRI scans to minimize the potential effects of the phase encoding polarities. The same averaging process was performed for these parametric maps calculated from the second LR and the second RL rsfMRI scans. In the end, each subject had two mean BEN maps (mdBEN1 and mdBEN2), two STD maps (STD_BEN1 and STD_BEN2), and two CV maps (CV_BEN1 and CV_BEN2). In addition, each subject had two static BEN maps: one was the average of the static maps calculated from the first LR and RL rsfMRI scans (msBEN1); the other was the average from the second LR and RL rsfMRI scans (msBEN2).

Statistical analysis.

Temporal fluctuations of BEN were first examined through the STD_BEN1, STD_BEN2, CV_BEN1, and CV_BEN2 maps. Their associations with biological measures (age and sex) and neurobehavioral measures (fluid intelligence and functional task performance) and education years were examined with multiple regression analysis. Specifically, a multiple regression model was built for each type of maps at each voxel using the map intensity at that voxel from all subjects as the dependent variable. Independent variables included age, sex, education years for the age/sex/education association analyses. A separate regression model including age, sex, and the PMT score as the independent variables was built for the BEN fluctuations vs fluid intelligence correlation analysis. For each functional task performance, an independent regression model including age, sex, and the task performance measure was used to assess the corresponding BEN fluctuations vs functional task

performance correlation. The model was built and estimated using SPM (https://www.fil.ion.ucl.ac.uk/spm/). The corresponding age/sex/education/fluid intelligence/task performance associations were statistically assessed through a contrast analysis with 1 for the interested variable and 0 for the other independent variables. The above analyses were repeated for mdBEN1, mdBEN2, msBEN1, and msBEN2.

The voxelwise significance threshold for assessing each of the association analysis results was defined by $p<0.05$. Multiple comparison (across voxels) correction was performed with the family wise error theory (Nichols and Hayasaka, 2003).

Results

The GPU-based implementation of BENtbx was 10-fold faster than the original version. But it still took roughly 10 days to calculate the static BEN maps for all 1023 subjects. The dynamic BEN mapping took about 40 days. Only 862 had all 4 rsfMRI scans, and the following analyses were based on the BEN maps of the 862 subjects. Fig. 2 shows the across subject average mdBEN maps (2A-2D), average STD_BEN (2E, 2F), average CV_BEN maps (2G, 2H) of the two sessions (each session containing a LR and a RL scan) of all 862 subjects. The across subject average BEN maps from the static BEN mapping (msBEN1 and msBEN2 as shown in Fig. 2A and 2B) were very similar to the average mdBEN maps (Fig. 2C and 2D), although the intensity differed due to the significant difference of the time series length (1200 for the static BEN mapping vs 300 for the dynamic BEN mapping). Gray matter (GM) showed lower BEN than white matter (WM) ($p<1e-15$, two tailed two sample t-test on the GM and WM BEN values), and regions in the default mode networks (DMN) had lower BEN than the rest of the brain ($p<1e-10$, two tail two sample t-test for all subjects); both findings are consistent with our previous study. Dynamic BEN showed inhomogeneous fluctuations across the brain with higher fluctuations in WM, visual cortex, and motor cortex ($p<1e-10$, one-way ANOVA) (Fig. 2E, 2F). In relative to the mean BEN, dynamic BEN showed very high temporal stability as measured by the CV (<0.032 in the whole brain, Fig. 2G, 2H. Data with CV <1 is often considered low variation).

We then assessed the effects of age and sex on BEN and its variations. We also examined the associations between cognition and BEN as well as its variations. The results from the BEN maps calculated from the entire 1200 time points and then averaged across the LR and RL scans were highly similar to those from the mean BEN maps of the dynamic BEN image series. Therefore, the results shown below were based on the static BEN mapping results (msBEN1 and msBEN2) only. Fig. 3 shows the test-retest stability of BEN as calculated by the intra-class correlation (ICC) (Shrout and Fleiss, 1979) between msBEN1 and msBEN2 at each voxel across all subjects. ICC is between −1 and 1 with 1 means fully repeatable. Usually ICC>0.3 can be treated as reliable. Using ICC>0.3, we can see from Fig. 3 that BEN is reliable across the entire brain cortex. Based on this reliability analysis result and the fact of that the association analysis results based on the mean of the first LR and the first RL rsfMRI scans (msBEN1) or the mean of the second LR and the second RL scans (msBEN2) were very similar, we chose to show the results based on the mean BEN of the first LR and RL scans (msBEN1) only.

Fig. 4 shows the association maps of BEN to age, sex, education years, and fluid intelligence. Resting BEN was significantly correlated with age (Fig. 4A) in the prefrontal executive control network (ECN, consisting of the lateral prefrontal cortex, the posterior parietal cortex, the frontal eye fields, and part of the dorso-medial prefrontal cortex) and the frontal-temporal-parietal DMN. Determinations of ECN and DMN were based on previous publication about the two highly repeatable resting state networks(Beckmann et al., 2005; Biswal, 2012; Damoiseaux et al., 2006; Meindl et al., 2010; Shehzad et al., 2009; Smith et al., 2013). Women showed higher BEN in visual cortex, motor area, and some part of precuneus (Fig. 4B) than men. Longer education years were associated with decreased BEN in ECN and DMN (Fig. 4C). In Fig 4D, higher fluid intelligence was associated with lower BEN in part of ECN and DMN. Educations years were significantly correlated with fluid intelligence ($r=.35$, $p=4.4e-28$).

Fig 5 shows the associations of resting BEN to functional task performance. BEN in DMN and part of ECN was negatively correlated with better performance during performing working memory (Fig. 5A), language (Fig. 5B), and relational tasks (Fig. 5C). Temporal STD of BEN showed no significant age and sex effects and no significant correlations to education years, fluid intelligence, and task performance. Task performance indices were significantly ($p<6e-40$) correlated ($r=0.39, 0.40, 0.81$ for the working memory vs language, working memory vs relational, language vs relational task performance correlation, respectively).

Discussion

The major focus of this study was to examine the potential neurocognitive correlates of LRTC measured by rsfMRI entropy. Based on the observations of that resting state brain activity is non-specific to any cognitive function, we hypothesized that resting BEN may be linked to general cognitive capability as reflected by fluid intelligence and performance of functional tasks. We further postulated the potential link of BEN to these general capabilities to be observed in DMN/ECN because the two networks have been consistently shown to be active during task performing or at rest. To ensure the study rigor and reliability, we chose the HCP data set, which is thus far the largest one acquired at the single site using the same MR scanner with four repeated rsfMRI scans, each with 1200 timepoints. We first examined the potential transit fluctuations of BEN using a sliding window-based dynamic BEN mapping method. Our results showed that BEN was stable across the entire acquisition time with minor temporal variations, which did not show any significant correlation to age, sex, education, and neurocognitive measures after multiple comparison corrections. We then assessed the neurocognitive associations of resting BEN. Our results showed that BEN in DMN and ECN increases with age but decreases with years of education; women had higher BEN than men in the cortical area; BEN in DMN and ECN was negatively correlated with fluid intelligence and task performance for all of the three assessed cognitive tasks.

The high temporal stability of resting BEN across many different timepoints is consistent with the high test-retest reproducibility of BEN shown in our previous study (Wang et al., 2014), suggesting BEN as a reliable brain activity metric. The finding of no significant correlation (after multiple comparison corrections) between the variability of transit BEN to

age and cognitive functions further suggest that the apparent BEN derived from rsfMRI is stable across age and that the small variations have no significant neurocognitive meanings at least for the healthy young adults.

Our major findings were the negative correlations between BEN in DMN/ECN and general functionality (reflected by fluid intelligence and task performance) and education. The negative education years vs DMN/ECN BEN correlation was consistent with our most recent study of BEN in normal aging and Alzheimer's Disease (Wang, 2020). These associations support our hypothesis about the potential role of resting state brain activity and its LRTC/BEN in general cognitive capability: resting state brain activity in DMN/ECN may create or maintain a reserve of brain functionality and lower BEN (higher LRTC) indicates a larger capacity of the potential reserve. The reason for postulating this potential link is that education is a widely used proxy of brain reserve and brain reserve is a well-studied model of general cognitive capability for compensating cognitive impairment caused by neuropathological brain damages (Stern, 2006). In young healthy subjects, there is no pathological brain damage related brain dysfunction to compensate. Likely the major role of the latent brain reserve is to facilitate general intelligence and general functionality. Our BEN vs fluid intelligence and functional task performance association analyses served to test this postulation. Fluid intelligence is a surrogate measure of general intelligence as it needs more than the sum of the learned and specialized skills for solving newly encountered problems (Horn and Cattell, 1967). The negative correlations between BEN and three different task performance suggest that resting BEN is non-specific to a particular domain function, proving its hypothetical role in general functionality. Education has been shown to be moderately correlated with general intelligence in young healthy individuals (Ritchie and Tucker-Drob, 2018) as we also observed in this study. However, in additional analysis (data not shown), we included education years and PMAT scores in the same model. By covarying out the education effects, we still observed similar BEN vs fluid intelligence association patterns though the suprathreshold clusters became slightly smaller. In other words, BEN is negatively correlated to fluid intelligence independent of education.

Our hypothesis about the latent functionality reserve and resting state activity was extended from the existing speculations that resting state brain activity plays a role in maintaining and facilitating brain functions such as language, social interaction, and memory (Raichle, 2006; Raichle and Gusnard, 2002; Raichle et al., 2001). The major difference between our hypothesis and the existing literature is the generality of the facilitation function of the resting state activity. We would argue that resting state brain activity backbones the general intelligence which is more than a summation of specific brain functions. This hypothesis was evidenced by the associations of resting BEN to general intelligence measured by fluid intelligence and education years.

Our association analysis results unanimously highlighted DMN and ECN, which is consistent with the well-known phenomenon that DMN and ECN (also called task positive network in (Shulman et al., 1997)) are two major brain circuits that are both active either during task performance (G. L. Shulman, 1997; Shulman et al., 1997) or at rest (Beckmann et al., 2005; Greicius et al., 2003). In previous studies, DMN and ECN were revealed as two separate but negatively correlated brain networks through the inter-regional signal

coherence. By contrast, DMN and ECN were identified as a single circuit based on LRTC of each voxel's time series. In other words, our results may suggest that DMN and ECN may represent one unified brain circuit underlying the general intelligence and general functionality of the brain. This postulation does not exclude the value of separating them into two networks based on inter-regional correlations but rather highlights the potential unification of them in terms of the non-directional temporal coherence. Since entropy is also a measure of information, an alternative view to understand this possible unification can be that resting state activity in these two networks presents equal information for assessing the latent brain function reserve, and it is that information/entropy capacity that differentiate them from other parts of the brain.

Resting brain activity has been shown to be predictive of human behavior (Chén et al., 2019; Li et al., 2013) or brain activation during functional task performance regional inter-voxel correlations(Cohen et al., 2020; Hampson et al., 2006; Liu et al., 2011; Tavor et al., 2016; Tian et al., 2012; Zou et al., 2013). These studies are mostly derived from inter-regional functional connectivity and often found different brain regions showing rest vs task or rest vs behavior associations. By contrast, our results consistently revealed the unified DMN/ECN area, which should be considered complementary to the existing rest vs task or rest vs cognition association literature.

Age effects identified in this study was consistent with the aging effects and the positive correlations between BEN and AD pathological deposition in healthy elderly people in our recently published paper(Wang, 2020). Guided by the second thermodynamic law, entropy of the brain tends to increase with age as tissues face more structural and functional deteriorations when they become older (Drachman, 2006; Hayflick, 2004). Entropy of resting brain activity has been shown to increase with age (Yao et al., 2013). Our study differed from theirs by using a different entropy calculation algorithm and by highlighting BEN in DMN and ECN. While the unfortunate aging-related entropy increase seems unavoidable, results of this paper and our recent publication(Wang, 2020) showed a negative correlation between education years and DMN BEN, suggesting a plausible way of reducing resting BEN through extended education and learning. In a recent study, our group showed that beneficial focal stimulations via transcranial magnetic stimulations can reduce local BEN(Donghui Song, 2017). In line with that neuromodulational effects, the education effects on resting BEN revealed in this paper and our recent publication (Wang, 2020) suggests that resting BEN may be modifiable, which is of particular interest for future brain disease studies.

Higher BEN in women was found in most of the brain cortices. Some of the sex effects were reported before (Li et al., 2016) but the spatial distribution is substantially bigger in this study. Since our BEN mapping results showed that lower BEN in frontal and parietal regions are associated with better fluid intelligence and functional task performance, higher cortical BEN in women suggests that women had worse performance of fluid intelligence test and functional task. To test this postulation, we assessed sex difference of the various neurobehavior scores available from the HCP database. We found that men had higher fluid capability than women as measured by the PMAT24 ($p=2e-6$), card sorting ($p=0.0017$), flanker test (also an measure of conflict solving, $p=0$); men had higher total cognitive score

(p=0.0001), picture vocabulary test (for crystal capability, p=0.0001) and total crystal capability score (p=5e-6); men performed better than women in language task (p=0), working memory task (p=0). These cognitive sex differences support the postulation given above and are consistent with the general literature (Đapo and Kolenović-Đapo, 2012; Halpern, 2013; Steinmayr et al., 2010). While we do not know the exact reason for the consistent sex differences, they might be contributed by genetic, hormonal, and environmental effects(Cosgrove et al., 2007), or even sleep (our additional analysis found that women had worse sleep quality (measured by Pittsburg Sleep Quality index, p=0.04). Future work is necessary to further delineate the reasons for the profound sex difference in BEN.

It is worth to note that resting-state fMRI is often contaminated by physiological noise such as respiration and heart rate variations (Birn et al., 2006; Birn et al., 2008; Chang et al., 2009; Chen et al., 2020; Kassinopoulos and Mitsis, 2019). Because the low frequency nature of these confounds, the high sampling rate of the multi-band sequence used in HCP allowed filtering out part of them. The data used in this study was processed by HCP using low-pass filtering and physiology noise removing steps including white matter and CSF signal regression (Behzadi et al., 2007) and independent component analysis-based denoising(Salimi-Khorshidi et al., 2014), which have been demonstrated to be able to substantially remove the physiological noise. Nevertheless, the residuals of those noise could still affect entropy mapping based rsfMRI, meaning that the apparent BEN might be still contaminated by physiological noise. Given the fact of that the DMN/ECN BEN patterns were unanimously identified in nearly all association analyses and physiological noise contamination is unlikely correlated to those biological and cognitive measures uniformly, it is reasonable to argue that the potential physiological contaminations to the main findings if there exist should be minimal. In a recent publication (Wang, 2020) we calculated BEN using the multi-site rsfMRI data from the Alzheimer's Disease Neuroimaging Initiative (ADNI). Since the ADNI rsfMRI data were acquired with the traditional gradient echo weighted echo planar imaging sequence that has much lower signal-to-noise-ratio and lower temporal resolution than the multi-band sequence used in the HCP, the level of physiological contaminations to the acquired rsfMRI should be very different from those in the HCP data. The residual contaminations if exist after processing should also be much different. But we still observed similar DMN BEN vs age and education correlations to those identified in this paper, which further release the concern of the physiological contaminations to BEN and the corresponding neurocognitive correlates. Another concern is the outliers, which can induce artificial large correlation coefficients using the moment-based Pearson Correlation Analysis. This concern was partially alleviated by the use of large samples. By examining the scatter plots between regional BEN and the biological/behavioral scores (see Supplementary Materials), we did not find obvious outliers in neither BEN nor the scores.

Regarding dynamic BEN mapping, parameters include the length of the dynamic BEN assessment window and the gap between adjacent assessment window may yield different results. It would be interesting to evaluate the variations due to the choice of these parameters. However, the computation time would be too excessive to take. As the variations are systematic to all subjects, we do not expect to see much difference regarding the image

pattern of the mean and std of the dynamic BEN images and their associations with age, sex, education, and neurocognitive measures.

Conclusion

In conclusion, the long rsfMRI time series from a large cohort of healthy subjects in the HCP proved BEN is a temporally stable brain activity measure. Resting BEN is associated with fluid intelligence and broad functionality. BEN in DMN/ECN may be assessed as a proxy for characterizing the potential functional reserve which may be improved by education and may result in better brain function.

Supplementary Material

Refer to Web version on PubMed Central for supplementary material.

Acknowledgements

The research effort involved in this study was supported by NIH/NIA R01 AG060054, AG060054-02S1, and by the support of the University of Maryland, Baltimore, Institute for Clinical & Translational Research (ICTR) and the National Center for Advancing Translational Sciences (NCATS) Clinical Translational Science Award (CTSA) grant number 1UL1TR003098. Both imaging and behavior data were provided by the Human Connectome Project, WU-Minn Consortium (Principal Investigators: David Van Essen and Kamil Ugurbil; 1U54MH091657) funded by the 16 NIH Institutes and Centers that support the NIH Blueprint for Neuroscience Research; and by the McDonnell Center for Systems Neuroscience at Washington University in St. Louis. The authors thank the Human Connectome Project for open access to its data and thank Brigitte Pocta for editing the manuscript. Part of the literature review in Introduction was generously provided by Prof Karl J. Friston.

References

Albert MS, Jones K, Savage CR, Berkman L, Seeman T, Blazer D, Rowe JW, 1995. Predictors of cognitive change in older persons: MacArthur studies of successful aging. Psychology and aging 10, 578. [PubMed: 8749585]

Barch DM, Burgess GC, Harms MP, Petersen SE, Schlaggar BL, Corbetta M, Glasser MF, Curtiss S, Dixit S, Feldt C, Nolan D, Bryant E, Hartley T, Footer O, Bjork JM, Poldrack R, Smith S, Johansen-Berg H, Snyder AZ, Van Essen DC, Consortium WU-MH, 2013. Function in the human connectome: task-fMRI and individual differences in behavior. NeuroImage 80, 169–189. [PubMed: 23684877]

Beckmann CF, DeLuca M, Devlin JT, Smith SM, 2005. Investigations into resting-state connectivity using independent component analysis. Philos Trans R Soc Lond B Biol Sci 360, 1001–1013. [PubMed: 16087444]

Behzadi Y, Restom K, Liau J, Liu TT, 2007. A component based noise correction method (CompCor) for BOLD and perfusion based fMRI. NeuroImage 37, 90–101. [PubMed: 17560126]

Bilker WB, Hansen JA, Brensinger CM, Richard J, Gur RE, Gur RC, 2012. Development of abbreviated nine-item forms of the Raven's standard progressive matrices test. Assessment 19, 354–369. [PubMed: 22605785]

Binder JR, Gross WL, Allendorfer JB, Bonilha L, Chapin J, Edwards JC, Grabowski TJ, Langfitt JT, Loring DW, Lowe MJ, Koenig K, Morgan PS, Ojemann JG, Rorden C, Szaflarski JP, Tivarus ME, Weaver KE, 2011. Mapping anterior temporal lobe language areas with fMRI: a multicenter normative study. NeuroImage 54, 1465–1475. [PubMed: 20884358]

Birn RM, Diamond JB, Smith MA, Bandettini PA, 2006. Separating respiratory-variation-related fluctuations from neuronal-activity-related fluctuations in fMRI. NeuroImage 31, 1536–1548. [PubMed: 16632379]

Birn RM, Smith MA, Jones TB, Bandettini PA, 2008. The respiration response function: the temporal dynamics of fMRI signal fluctuations related to changes in respiration. NeuroImage 40, 644–654. [PubMed: 18234517]

Biswal BB, 2012. Resting state fMRI: a personal history. NeuroImage 62, 938–944. [PubMed: 22326802]

Buzsáki G, Draguhn A, 2004. Neuronal oscillations in cortical networks. Science 304, 1926–1929. [PubMed: 15218136]

Cattell RB, 1963. Theory of fluid and crystallized intelligence: A critical experiment. Journal of educational psychology 54, 1.

Chang C, Cunningham JP, Glover GH, 2009. Influence of heart rate on the BOLD signal: the cardiac response function. NeuroImage 44, 857–869. [PubMed: 18951982]

Chen JE, Lewis LD, Chang C, Tian Q, Fultz NE, Ohringer NA, Rosen BR, Polimeni JR, 2020. Resting-state "physiological networks". NeuroImage 213, 116707. [PubMed: 32145437]

Chén OY, Cao H, Reinen JM, Qian T, Gou J, Phan H, De Vos M, Cannon TD, 2019. Resting-state brain information flow predicts cognitive flexibility in humans. Scientific Reports 9, 1–16. [PubMed: 30626917]

Chen X, Solomon I, Chon K, 2005. Comparison of the use of approximate entropy and sample entropy: applications to neural respiratory signal. Conference proceedings : … Annual International Conference of the IEEE Engineering in Medicine and Biology Society. IEEE Engineering in Medicine and Biology Society. Conference 4, 4212–4215.

Cohen AD, Chen Z, Parker Jones O, Niu C, Wang Y, 2020. Regression-based machine-learning approaches to predict task activation using resting-state fMRI. Human Brain Mapping 41, 815–826. [PubMed: 31638304]

Cosgrove KP, Mazure CM, Staley JK, 2007. Evolving knowledge of sex differences in brain structure, function, and chemistry. Biological psychiatry 62, 847–855. [PubMed: 17544382]

Damoiseaux JS, Rombouts SARB, Barkhof F, Scheltens P, Stam CJ, Smith SM, Beckmann CF, 2006. Consistent resting-state networks across healthy subjects. Proc Natl Acad Sci U S A 103, 13848–13853. [PubMed: 16945915]

Đapo N, Kolenović-Đapo J, 2012. Sex differences in fluid intelligence: Some findings from Bosnia and Herzegovina. Personality and Individual differences 53, 811–815.

Dean HL, Hagan MA, Pesaran B, 2012. Only coherent spiking in posterior parietal cortex coordinates looking and reaching. Neuron 73, 829–841. [PubMed: 22365554]

Deco G, Jirsa VK, 2012. Ongoing Cortical Activity at Rest: Criticality, Multistability, and Ghost Attractors. Journal of Neuroscience 32, 3366–3375. [PubMed: 22399758]

Donghui Song DC, Jian Zhang, Qiu Ge, Yu-Feng Zang, Ze Wang, 2019. Associations of Brain Entropy (BEN) to Cerebral Blood Flow and fractional Amplitude of Low-Frequency Fluctuations in the Resting Brain. Brain imaging and behavior 13, 486–1495.

Donghui Song WP, Jian Zhang, Yuanqi Shang, Ze Wang, 2017. Decreased brain entropy by 20 Hz rTMS on the left dorsolateral prefrontal cortex. Annual meeting of International Congress of MRI, Seoul, Korea.

Drachman DA, 2006. Aging of the brain, entropy, and Alzheimer disease. Neurology 67, 1340–1352. [PubMed: 17060558]

Drobyshevsky A, Baumann SB, Schneider W, 2006. A rapid fMRI task battery for mapping of visual, motor, cognitive, and emotional function. NeuroImage 31, 732–744. [PubMed: 16488627]

Fries P, 2005. A mechanism for cognitive dynamics: neuronal communication through neuronal coherence. Trends Cogn Sci 9, 474–480. [PubMed: 16150631]

Fries P, 2015. Rhythms for cognition: communication through coherence. Neuron 88, 220–235. [PubMed: 26447583]

Shulman GL, Corbetta JAF,M, Buckner RL, Miezin FM, Raichle ME, Petersen SE, 1997. Common blood flow changes across visual tasks: II. Decreases in cerebral cortex. J Cogn Neurosci 9, 648–663. [PubMed: 23965122]

Ganguli M, Ratcliff G, Huff J, Belle S, Kancel MJ, Fischer L, Seaberg EC, Kuller LH, 1991. Effects of age, gender, and education on cognitive tests in a rural elderly community sample: norms from the

Monongahela Valley Independent Elders Survey. Neuroepidemiology 10, 42–52. [PubMed: 2062416]

Greicius MD, Krasnow B, Reiss AL, Menon V, 2003. Functional connectivity in the resting brain: A network analysis of the default mode hypothesis. Proceedings of the National Academy of Sciences 100, 253–258.

Halpern DF, 2013. Sex differences in cognitive abilities. Psychology press.

Hampson M, Driesen NR, Skudlarski P, Gore JC, Constable RT, 2006. Brain connectivity related to working memory performance. Journal of Neuroscience 26, 13338–13343. [PubMed: 17182784]

Hayflick L, 2004. Aging: The Reality: "Anti-Aging" Is an Oxymoron. The Journals of Gerontology Series A: Biological Sciences and Medical Sciences 59, B573–B578.

He BJ, 2011. Scale-free properties of the functional magnetic resonance imaging signal during rest and task. J Neurosci 31, 13786–13795. [PubMed: 21957241]

Horn JL, Cattell RB, 1967. Age differences in fluid and crystallized intelligence. Acta psychologica 26, 107–129. [PubMed: 6037305]

Jung RE, Haier RJ, 2007. The Parieto-Frontal Integration Theory (P-FIT) of intelligence: converging neuroimaging evidence. Behavioral and Brain Sciences 30, 135.

Kassinopoulos M, Mitsis GD, 2019. Identification of physiological response functions to correct for fluctuations in resting-state fMRI related to heart rate and respiration. NeuroImage 202, 116150. [PubMed: 31487547]

Li N, Ma N, Liu Y, He XS, Sun DL, Fu XM, Zhang X, Han S, Zhang DR, 2013. Resting-state functional connectivity predicts impulsivity in economic decision-making. J Neurosci 33, 4886–4895. [PubMed: 23486959]

Li Z, Fang Z, Hager N, Rao H, Wang Z, 2016. Hyper-resting brain entropy within chronic smokers and its moderation by Sex. Sci Rep 6, 29435. [PubMed: 27377552]

Liu X, Zhu XH, Chen W, 2011. Baseline BOLD correlation predicts individuals' stimulus-evoked BOLD responses. NeuroImage 54, 2278–2286. [PubMed: 20934521]

Lu K, Xu Y, Yin P, Oxenham AJ, Fritz JB, Shamma SA, 2017. Temporal coherence structure rapidly shapes neuronal interactions. Nat Commun 8, 13900. [PubMed: 28054545]

Meindl T, Teipel S, Elmouden R, Mueller S, Koch W, Dietrich O, Coates U, Reiser M, Glaser C, 2010. Test-retest reproducibility of the default-mode network in healthy individuals. Hum Brain Mapp 31, 237–246. [PubMed: 19621371]

Moeller S, Yacoub E, Olman CA, Auerbach E, Strupp J, Harel N, Ugurbil K, 2010. Multiband multislice GE-EPI at 7 tesla, with 16-fold acceleration using partial parallel imaging with application to high spatial and temporal whole-brain fMRI. Magn Reson Med 63, 1144–1153. [PubMed: 20432285]

Nichols TE, Hayasaka S, 2003. Controlling the Familywise Error Rate in Functional Neuroimaging: A Comparative Review. Statistical Methods in Medical Research 12, 419–446. [PubMed: 14599004]

Pesaran B, Pezaris JS, Sahani M, Mitra PP, Andersen RA, 2002. Temporal structure in neuronal activity during working memory in macaque parietal cortex. Nat Neurosci 5, 805–811. [PubMed: 12134152]

Raichle ME, 2006. Neuroscience. The brain's dark energy. Science 314, 1249–1250. [PubMed: 17124311]

Raichle ME, 2015. The restless brain: how intrinsic activity organizes brain function. Philos Trans R Soc Lond B Biol Sci 370.

Raichle ME, Gusnard DA, 2002. Appraising the brain's energy budget. Proceedings of the National Academy of Sciences of the United States of America 99, 10237–10239. [PubMed: 12149485]

Raichle ME, Gusnard DA, 2005. Intrinsic brain activity sets the stage for expression of motivated behavior. J Comp Neurol 493, 167–176. [PubMed: 16254998]

Raichle ME, MacLeod AM, Snyder AZ, Powers WJ, Gusnard DA, Shulman GL, 2001. A default mode of brain function. PNAS 98, 676–682. [PubMed: 11209064]

Raichle ME, Snyder AZ, 2007. A default mode of brain function: a brief history of an evolving idea. NeuroImage 37, 1083–1090. [PubMed: 17719799]

Raven J, 2000. The Raven's progressive matrices: change and stability over culture and time. Cognitive psychology 41, 1–48. [PubMed: 10945921]

Reinhart RMG, Nguyen JA, 2019. Working memory revived in older adults by synchronizing rhythmic brain circuits. Nat Neurosci 22, 820–827. [PubMed: 30962628]

Richman JS, Moorman JR, 2000. Physiological time-series analysis using approximate entropy and sample entropy. American journal of physiology. Heart and circulatory physiology 278, H2039–2049. [PubMed: 10843903]

Ritchie SJ, Tucker-Drob EM, 2018. How much does education improve intelligence? A meta-analysis. Psychological science 29, 1358–1369. [PubMed: 29911926]

Rubinov M, Sporns O, Thivierge JP, Breakspear M, 2011. Neurobiologically Realistic Determinants of Self-Organized Criticality in Networks of Spiking Neurons. Plos Computational Biology 7.

Saleh M, Reimer J, Penn R, Ojakangas CL, Hatsopoulos NG, 2010. Fast and slow oscillations in human primary motor cortex predict oncoming behaviorally relevant cues. Neuron 65, 461–471. [PubMed: 20188651]

Salimi-Khorshidi G, Douaud G, Beckmann CF, Glasser MF, Griffanti L, Smith SM, 2014. Automatic denoising of functional MRI data: combining independent component analysis and hierarchical fusion of classifiers. NeuroImage 90, 449–468. [PubMed: 24389422]

Shehzad Z, Kelly AMC, Reiss PT, Gee DG, Gotimer K, Uddin LQ, Lee SH, Margulies DS, Roy AK, Biswal BB, Petkova E, Castellanos FX, Milham MP, 2009. The resting brain: unconstrained yet reliable. Cereb Cortex 19, 2209–2229. [PubMed: 19221144]

Shrout PE, Fleiss JL, 1979. Intraclass correlations: uses in assessing rater reliability. Psychol Bull 86, 420–428. [PubMed: 18839484]

Shulman GL, Corbetta M, Buckner RL, Fiez JA, Miezin FM, Raichle ME, Petersen SE, 1997. Common Blood Flow Changes across Visual Tasks: I. Increases in Subcortical Structures and Cerebellum but Not in Nonvisual Cortex. J Cogn Neurosci 9, 624–647. [PubMed: 23965121]

Smith SM, Beckmann CF, Andersson J, Auerbach EJ, Bijsterbosch J, Douaud G, Duff E, Feinberg DA, Griffanti L, Harms MP, Kelly M, Laumann T, Miller KL, Moeller S, Petersen S, Power J, Salimi-Khorshidi G, Snyder AZ, Vu AT, Woolrich MW, Xu J, Yacoub E, Ugurbil K, Van Essen DC, Glasser MF, Consortium WU-MH, 2013. Resting-state fMRI in the Human Connectome Project. NeuroImage 80, 144–168. [PubMed: 23702415]

Song D, Chang D, Zhang J, Peng W, Shang Y, Gao X, Wang Z, 2018. Reduced brain entropy by repetitive transcranial magnetic stimulation on the left dorsolateral prefrontal cortex in healthy young adults. Brain imaging and behavior, 1–9. [PubMed: 28070745]

Steinmayr R, Beauducel A, Spinath B, 2010. Do sex differences in a faceted model of fluid and crystallized intelligence depend on the method applied? Intelligence 38, 101–110.

Stern Y, 2006. Cognitive reserve and Alzheimer disease. Alzheimer Dis Assoc Disord 20, 112–117. [PubMed: 16772747]

Stern Y, Arenaza-Urquijo EM, Bartrés-Faz D, Belleville S, Cantilon M, Chetelat G, Ewers M, Franzmeier N, Kempermann G, Kremen WS, 2018. Whitepaper: Defining and investigating cognitive reserve, brain reserve, and brain maintenance. Alzheimers Dement (Amst).

Stern Y, Gurland B, Tatemichi TK, Tang MX, Wilder D, Mayeux R, 1994. Influence of education and occupation on the incidence of Alzheimer's disease. JAMA 271, 1004–1010. [PubMed: 8139057]

Tagliazucchi E, Chialvo DR, Siniatchkin M, Amico E, Brichant JF, Bonhomme V, Noirhomme Q, Laufs H, Laureys S, 2016. Large-scale signatures of unconsciousness are consistent with a departure from critical dynamics. J R Soc Interface 13, 20151027. [PubMed: 26819336]

Tavor I, Parker Jones O, Mars RB, Smith SM, Behrens TE, Jbabdi S, 2016. Task-free MRI predicts individual differences in brain activity during task performance. Science 352, 216–220. [PubMed: 27124457]

Teki S, Chait M, Kumar S, Shamma S, Griffiths TD, 2013. Segregation of complex acoustic scenes based on temporal coherence. Elife 2, e00699. [PubMed: 23898398]

Thut G, Miniussi C, Gross J, 2012. The functional importance of rhythmic activity in the brain. Current Biology 22, R658–R663. [PubMed: 22917517]

Tian L, Ren J, Zang Y, 2012. Regional homogeneity of resting state fMRI signals predicts Stop signal task performance. NeuroImage 60, 539–544. [PubMed: 22178814]

Valenzuela MJ, Sachdev P, 2006. Brain reserve and dementia: a systematic review. Psychological medicine 36, 441. [PubMed: 16207391]

Van Essen DC, Smith SM, Barch DM, Behrens TE, Yacoub E, Ugurbil K, Consortium WU-MH, 2013. The WU-Minn Human Connectome Project: an overview. NeuroImage 80, 62–79. [PubMed: 23684880]

Wang Z, 2012a. Characterizing Resting Brain Information using Voxel-based Brain Information Mapping (BIM). 2012 Annual Meeting of the Organization for Human Brain Mapping, Beijing, China.

Wang Z, 2012b. Stable and Self-Organized Entropy in the Resting Brain. The Third Biennial Conference on Resting State Brain Connectivity, Magdeburg, Germany, p. 208.

Wang Z, 2020. Brain Entropy Mapping in Healthy Aging and Alzheimer's Disease. Front Aging Neurosci.

Wang Z, Li Y, Childress AR, Detre JA, 2014. Brain Entropy Mapping Using fMRI. PLoS One 9, e89948. [PubMed: 24657999]

Womelsdorf T, Fries P, Mitra PP, Desimone R, 2006. Gamma-band synchronization in visual cortex predicts speed of change detection. Nature 439, 733. [PubMed: 16372022]

Woolgar A, Parr A, Cusack R, Thompson R, Nimmo-Smith I, Torralva T, Roca M, Antoun N, Manes F, Duncan J, 2010. Fluid intelligence loss linked to restricted regions of damage within frontal and parietal cortex. Proceedings of the national academy of sciences 107, 14899–14902.

Xue SW, Yu Q, Guo Y, Song D, Wang Z, 2019. Resting-state brain entropy in schizophrenia. Compr Psychiatry 89, 16–21. [PubMed: 30576960]

Yao Y, Lu WL, Xu B, Li CB, Lin CP, Waxman D, Feng JF, 2013. The Increase of the Functional Entropy of the Human Brain with Age. Scientific Reports 3.

Zang YF, He Y, Zhu CZ, Cao QJ, Sui MQ, Liang M, Tian LX, Jiang TZ, Wang YF, 2007. Altered baseline brain activity in children with ADHD revealed by resting-state functional MRI. Brain & development 29, 83–91. [PubMed: 16919409]

Zhou F, Zhuang Y, Gong H, Zhan J, Grossman M, Wang Z, 2016. Resting State Brain Entropy Alterations in Relapsing Remitting Multiple Sclerosis. PLoS One 11, e0146080. [PubMed: 26727514]

Zou Q, Ross TJ, Gu H, Geng X, Zuo XN, Hong LE, Gao JH, Stein EA, Zang YF, Yang Y, 2013. Intrinsic resting-state activity predicts working memory brain activation and behavioral performance. Human Brain Mapping 34, 3204–3215. [PubMed: 22711376]

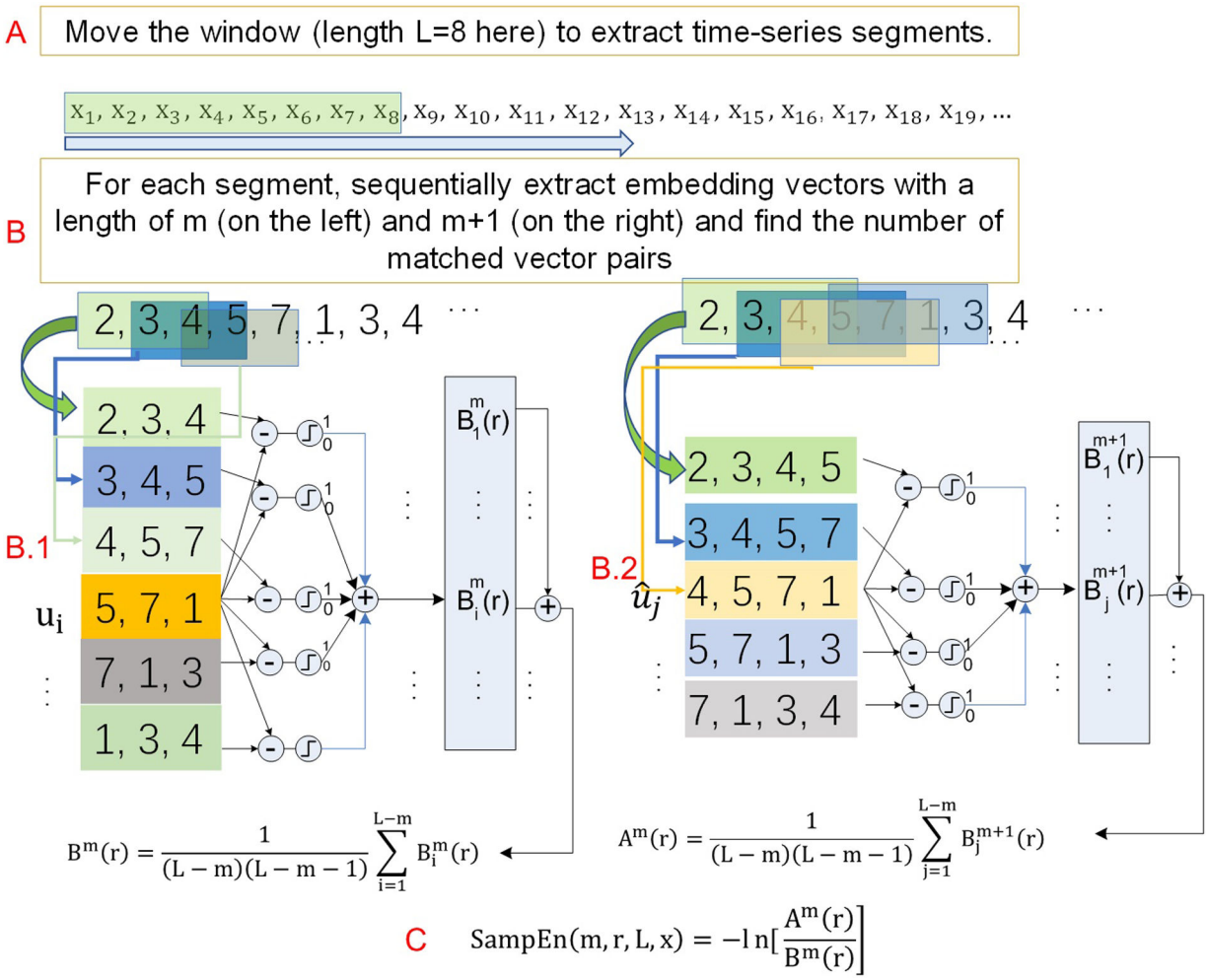

Fig. 1.

A scheme of the sliding window-based dynamic entropy calculation. A) A large time window is used to extract a sub-time series at N successive timepoints (N=8 here) from the original time series. The green box indicates the window slid to the n-th timepoint. B) The standard sample entropy formula is used to calculate entropy for the sub-time series extracted from A. B.1 and B.2 illustrate the embedding vector matching process for the embedding window length of m and m+1, respectively. The boxes in different color indicate the locations of the embedding vectors in the input time series—the sub-series from A).

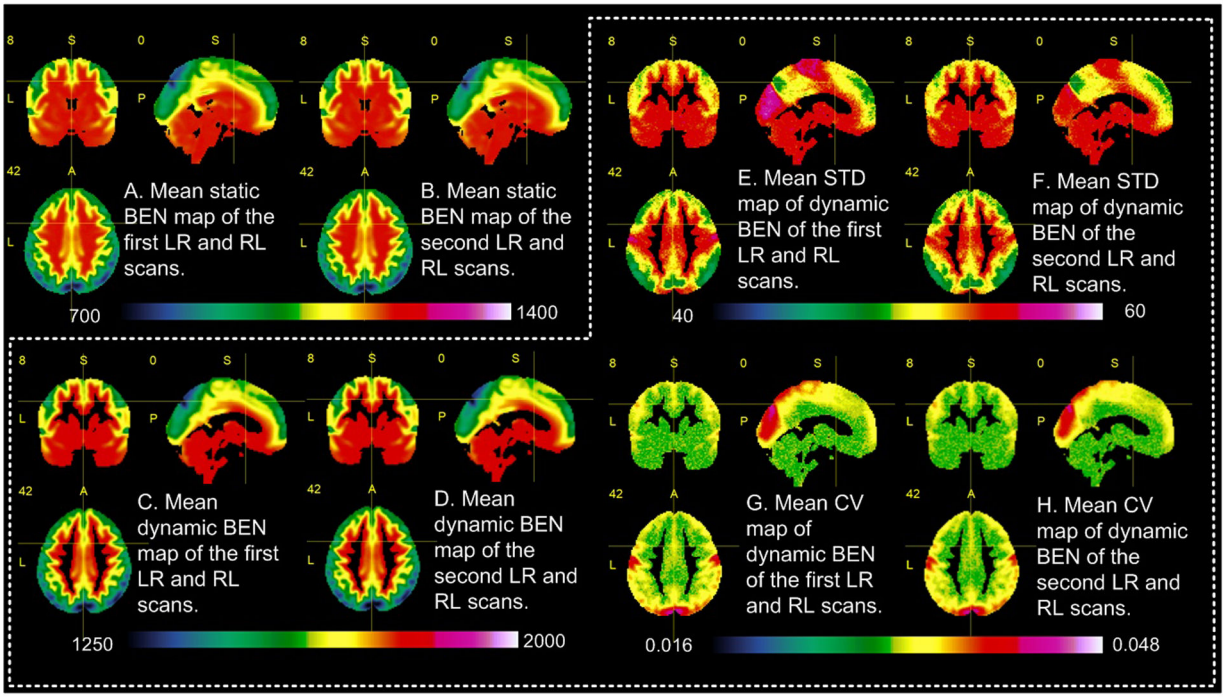

Fig. 2.

Across-subject (n=862) mean maps. A) and B) are the mean of individual subject's static BEN maps of the first LR and RL scans, and the second LR and RL scans, respectively. C) and D) are the mean of all subjects' average dynamic BEN maps of the first LR and RL scans, and the second LR and RL scans, respectively. E) and F) are the across-subject mean of the dynamic BEN STD. G) and H) are the mean CV map of the dynamic BEN.

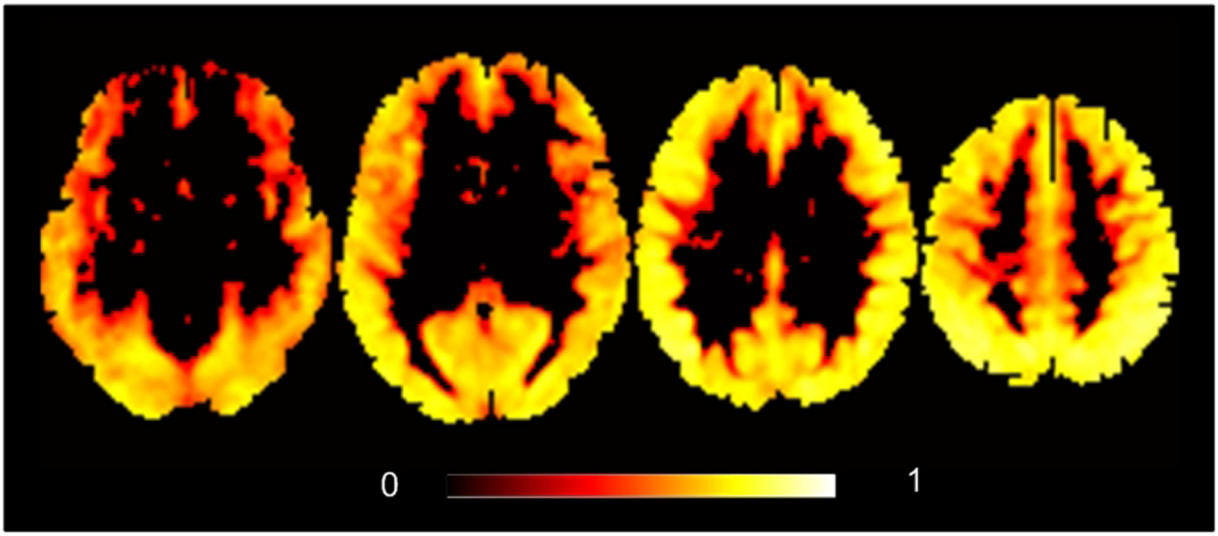

Fig. 3.
ICC of the static BEN maps (msBEN1 and msBEN2). Threshold was ICC>0.3.

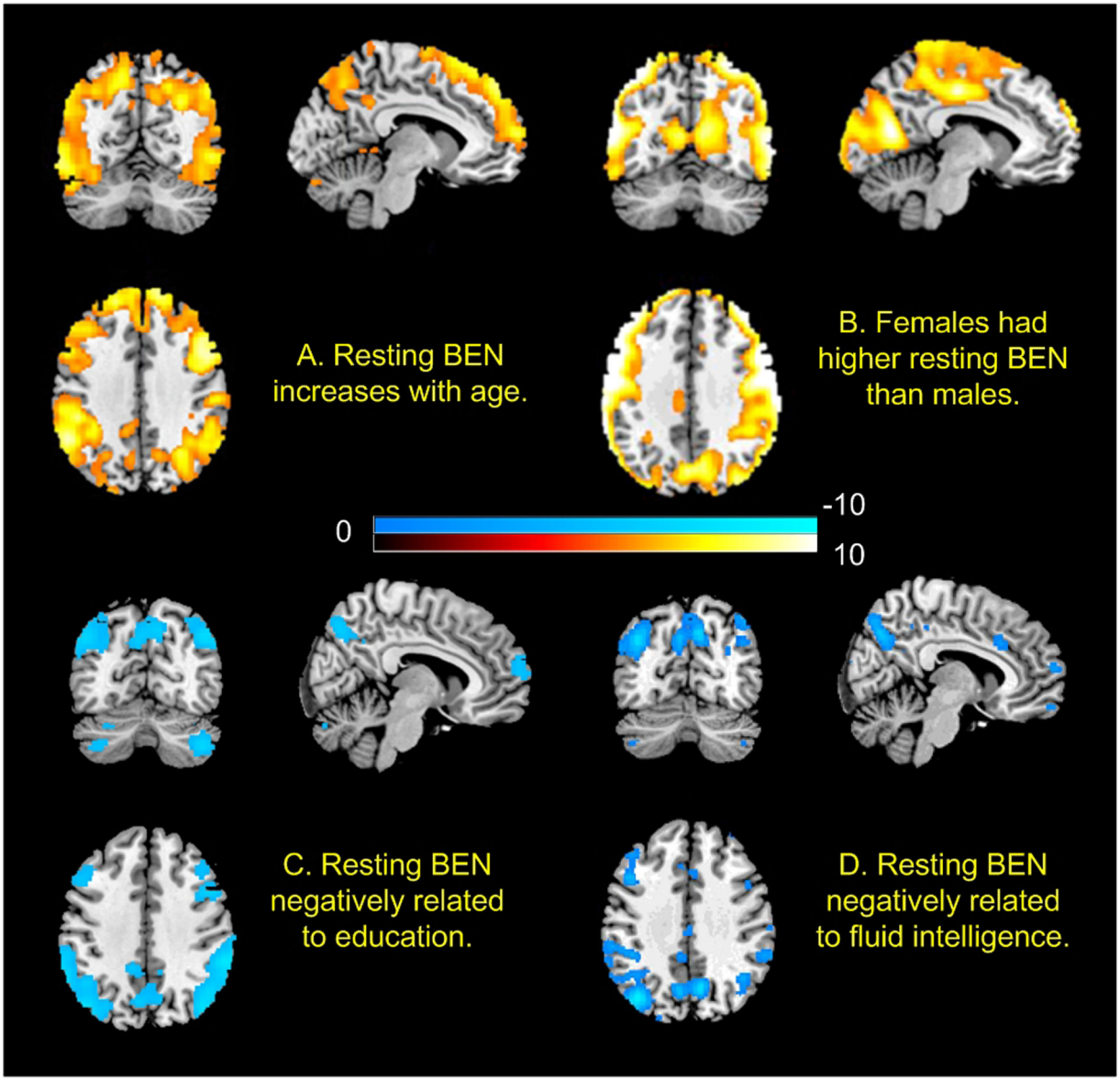

Fig. 4.

The age, sex, and education effects on resting BEN as well as the associations of resting BEN with fluid intelligence. n = 862. Statistical significance level was $p<0.05$ (FWE corrected). Red/blue colors indicate positive/negative correlations, respectively. Color bars indicate the t-values of the regression analyses (A, C, and D) and the two-sample t-test (B).

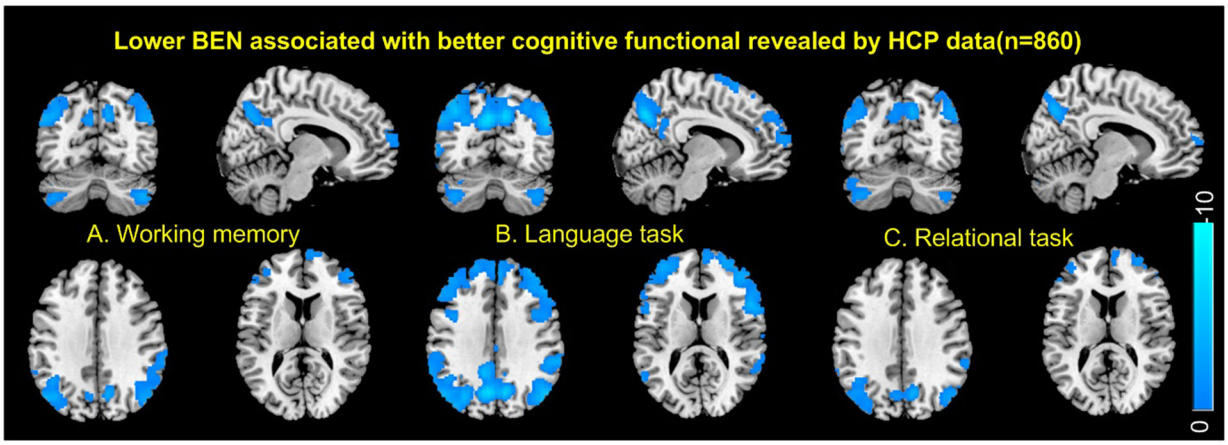

Fig. 5.

Resting BEN was negatively associated with task performance in A) working memory task, B) language task, C) relational task. Blue color indicates negative correlation. Statistical significance level was defined by $p<0.05$ (FWE corrected). Task performance was measured by the accuracy of item selection during the on-the-magnet fMRI tasks.